AGS Letter of Intent-Search for a Permanent Muon Electric Dipole Moment

R.M. Carey, J.P. Miller*, O. Rind, B.L. Roberts, L.R. Sulak

Boston University

R. Larsen, D.M. Lazarus, W. Meng,

W.M. Morse, C. Ozben, R. Prigl, Y.K. Semertzidis*

Brookhaven National Lab

V. Balakin, A. Bazhan, A. Dudnikov, B. Khazin, G. Sylvestrov

BINP, Novosibirsk

Y. Orlov

Cornell University

K. Jungmann

University of Heidelberg

P.T. Debevec, D.W. Hertzog

University of Illinois

E. Stephenson

Indiana University

F.J.M. Farley

Yale University

February 11, 2000

* Spokesperson

1 Abstract

We propose to modify the existing muon g-2 storage ring at the Brookhaven National Laboratory (BNL) to carry out a dedicated search for a permanent electric dipole moment (EDM) of the muon. In a stage-wise approach we aim for a sensitivity at a level of $10^{-24}\,\mathrm{e}\cdot\mathrm{cm}$. The experimental design exploits the strong motional electric field sensed by relativistic particles in a magnetic storage ring [1, 2]. As a key feature a novel technique has been invented in which the g-2 precession is compensated with radial electric field.

Contents

1 Abstract **2**

2 Introduction **2**

3 Motivation **5**

4 Experimental Overview **10**

4.1 Target and Beam Line 14

4.2 Weak Focusing Ring 15

4.3 Inflector 17

4.4 Storage Ring-Weak Magnetic Focusing 18

4.5 Storage Ring-Strong Magnetic Focusing 19

4.6 Storage Ring Lattice 20

4.7 Detectors 21

5 Sensitivity Level **23**

5.1 Calibration of Sensitivity 24

6 Systematic Errors **25**

6.1 Electrode alignment 27

6.2 Inclinometer 28

6.3 Deuteron Polarimeter 30

6.4 Pickup Electrode Measurement of Vertical Component of Electric Field . . 34

7 Cost and Schedule **36**

8 Summary **37**

2 Introduction

Unlike the magnetic dipole moment, the existence of a permanent electric dipole moment in a muon (or any other elementary particle) is a violation of time and parity symmetries, with the predicted value for the muon from the Standard Model, being well below the sensitivity of our proposed measurement. Therefore, a non-zero measurement of the muon EDM is unmistakable evidence of physics beyond the standard model. A detailed discussion of the merits of measuring the muon EDM is given in the theory section.

There is only one preferred direction for the muon, namely, the direction of its spin angular momentum. Consequently, any electric or magnetic moments must be either parallel or anti-parallel to this direction.

As is well-known, an external B-field will cause a torque on the muon, due to the presence of a non-zero magnetic moment, which tries to align the moment along the direction of $\vec{B}$. By virtue of its non-zero angular momentum, the magnetic moment precesses about the direction of the B-field instead of aligning with it. In complete analogy with the magnetic moment, if the EDM is non-zero, an external E-field will produce a torque on the muon which tries to align the EDM along $\vec{E}$. By virtue of its angular momentum, it precesses about the direction of the E-field rather than aligning with it.

In the presence of a uniform B-field, such as in the muon (g-2) storage ring, the muon travels in a circle at the cyclotron frequency about an axis parallel to $\vec{B}$ ($\hat{\mathbf{z}}$ axis). In the rest frame of the muon, there is both an E and a B-field from the Lorentz transformation, E^* and B^*. B^* causes the muon's spin to precess relative to its momentum at the rate

$$\vec{\omega}_a \approx a\frac{eB}{m}\hat{\mathbf{z}}$$

where $a = \frac{g-2}{2}$ is the anomalous magnetic dipole moment.

The E^*-field, which is the only source of net force in the muon rest frame, must be radially directed to cause the circular motion; any vertical component would cause the muon to change its vertical position, while any azimuthal component would increase or decrease the momentum. The E^*-field causes the muon spin to precess in a vertical plane with an axis directed along the radial E^*-field, according to

$$\vec{\omega}_\eta \approx \frac{\eta}{2}\frac{e\vec{\beta} \times \vec{B}}{m}$$

where $d = \eta\frac{e\hbar}{4mc}$ is the electric dipole moment.

The total precession frequency of the spin is the sum of these two terms

$$\vec{\omega} \approx \vec{\omega}_a + \vec{\omega}_\eta$$

In the absence of an EDM, $\vec{\omega}$ will be parallel to $\vec{B}$, so the muon will precess in the plane of the storage ring, perpendicular to $\vec{B}$. In the presence of a non-zero EDM, $\vec{\omega}$ will be tipped in the radial direction by the angle $\delta = tan^{-1}(\frac{\eta\beta}{2a})$, and ω will be increased over ω_a by the factor $\sqrt{1+\delta^2}$. Consequently the plane of spin rotation is no longer in the plane of the storage magnet. Relative to the momentum vector, in addition to the precession about the z-axis, the spin also bobs up and down vertically at the precession frequency.

The directions and energies of the decay electron are correlated to the muon spin direction. In particular, when the plane of spin precession is tipped out of the plane of the storage magnet the decay electrons will have average upward and downward momentum components as the muon spin bobs up and down. A measurement of the average vertical position of electrons striking the detectors will oscillate at the frequency ω. The magnitude of this oscillation is a direct measurement of the EDM. In addition, if the value of ω differs from the theoretically predicted value for ω_a, the difference could be attributed to the factor $\sqrt{1+\delta^2}$, which provides a second, indirect means of measuring the EDM, under the assumption that any deviation from theory is entirely due to the EDM. These are the principles behind the two methods of determining the EDM which were used by the CERN muon (g-2) experiments in the 1970's.

The reported limit from the last CERN experiment is $3.7 \pm 3.4 \times 10^{-19}\,\mathrm{e \cdot cm}$. The error is the combined result of the statistical and systematic errors:

- Statistical: $\pm 2.7 \times 10^{-19}\,\mathrm{e \cdot cm}$
- Systematic: $\pm 2 \times 10^{-19}\,\mathrm{e \cdot cm}$

There are at least two sources of systematic errors when the spin is allowed to precess: 1) The center of the muon population is not exactly aligned with the geometric center of the detectors which results in an up-down modulation of the average decay positron position with the g-2 frequency. 2) As the muon spin precesses the decay positrons travel through different magnetic and electric fields before they reach the detector which again results in an up-down modulation of the average decay positron position with the g-2 frequency.

The novel approach of the new experiment is to cancel the muon's spin precession about the vertical axis by applying an external radial E-field in addition to the vertical B-field. The torque of the E-field acting on the magnetic moment cancels the torque due to the magnetic field. Only the precession due to the EDM remains, at the rate ω_η about the radial direction (with a small change in ω_η due to the applied E-field). Since there is now no precession in the horizontal plane, any vertical precession angle can accumulate with time, amplifying the effect due to the EDM and makes possible the elimination of the above systematic errors.

However, the introduction of the E-field has its own systematic errors associated with it, namely the average E-field direction needs to be known very accurately with respect to the average B-field.

This Letter of Intent is largely based on the old one on the muon EDM [1]. The main differences are:

1. The introduction of an inclinometer, i.e. a system of measuring in situ the misalignment of the average radial electric field direction (which is used to cancel the spin motion of the muon) and the direction of the average dipole magnetic field. The requirement of this experiment for a sensitivity to the muon Electric Dipole Moment at the 1×10^{-24} e $\cdot$ cm level is that the average direction of the E-field needs to be orthogonal to the average direction of the B-field to ± 10 nrad or known to that level of accuracy. This is done by injecting polarized deuterons in the ring with two methods described in the systematic errors section.

2. The introduction of a monitoring system for the alignment of the electric and magnetic field directions by a set of laser interferometers between the deuteron runs. This is also described in the systematic errors section.

3. The proposed improvement on the muon EDM is more than five orders of magnitude over its present limit. We have now taken a new stepwise approach with well defined goals:

   - First we run with polarized deuterons without modifying the pole pieces of the g-2 ring. At this point we measure the misalignment (with deuterons) and time stability (with laser interferometers) of the $\vec{E}$ field and the orthogonal plane to $\vec{B}$ fields to ± 10 nrad.
   - Next we run with muons and set a first limit of order of $10^{-22}\,\mathrm{e}\cdot\mathrm{cm}$ controlling the systematics 100 times better, i.e. at the $10^{-24}\,\mathrm{e}\cdot\mathrm{cm}$ level.
   - Next we modify the g-2 pole pieces to store more muons and reach $10^{-23}\,\mathrm{e}\cdot\mathrm{cm}$ level sensitivity.
   - If the claimed sensitivities can be accomplished and the experiment is statistics limited then we will apply the techniques pioneered by the muon collider, muon storage ring and the meco collaborations to improve the limit down to $10^{-24}\,\mathrm{e}\cdot\mathrm{cm}$ by injecting 100 times more muons.

Further improvements over the $10^{-24}\,\mathrm{e}\cdot\mathrm{cm}$ will depend on both statistics, i.e. the availability of intense muon sources (like those assumed for the muon storage rings), and systematics, i.e. the stability of the $\vec{E}$ and $\vec{B}$ fields with time.

3 Motivation

The standard model of particle physics is a very successful theoretical framework, which describes all confirmed observations to date. Even surprising recent observations in neutrino physics could be possibly accommodated with small modifications. However, the model leaves important questions concerning the physical nature of observed processes unexplained, although it provides an accurate description of them. Among the not yet understood phenomena are the reasons for parity violation, the particle masses, the violation of the CP symmetry, the combined charge conjugation (C) and parity (P) transformation, etc. CP violation is the only known mechanism that could explain the matter antimatter

asymmetry found in the universe. In order to obtain a deeper insight, speculative models have been suggested which often are connected to observable deviations from standard theory predictions, particularly violations of assumed symmetries or yet unknown properties of particles. The spectrum of these theories includes super symmetry [3, 4], left-right symmetry [5], multi Higgs scenarios [6, 7] and many other important approaches. This strongly motivates sensitive searches for forbidden decays, e.g. the lepton number violating muon electron conversion [8] , the decay $\mu \rightarrow e\gamma$ [9] and precise measurements of particle characteristics such as the muon magnetic anomaly [10].

A fundamental particle is described by only a few parameters such as its mass, its intrinsic angular momentum, its electric charge (electric monopole moment), its magnetic dipole moment, and a set of conserved quantum numbers, like lepton flavor [11]. A permanent EDM is not known for any of them. It would violate both parity (P) and time reversal (T) invariance. If CPT is assumed to be a valid unbroken symmetry, a permanent EDM would hence be a signature of CP violation [12, 3].

The standard model of particle physics predicts a CP violating EDM in fundamental particles at the multi loop level of amplitude more than five orders of magnitude below the sensitivity of present experiments [13] (see Table 1). Therefore searches for a permanent particle EDM render excellent opportunities to test models beyond standard theory where in some cases they predict effects as large as the presently known experimental bounds. Despite the non-observation of a positive EDM signal such research has nevertheless been most successful in steering the development of theoretical particle physics over many decades and also was the incentive for the ever increasing precision in the experiments themselves. The absence of any observed finite EDM for the neutron, for example, has disfavored more speculative models than any other experimental approach so far [14].

Searches for EDMs have been performed with highest sensitivity for electrons (e) and neutrons (n). Further there are experimental limits for muons (μ), taus (τ) and protons

(p) (Table 1). The experimental techniques include beams of neutral atoms, molecular beams, stored neutrons and stored charged particles. In heavy atoms and particularly in polar molecules there are substantial enhancement factors due to the utilization of the rather strong internal electric fields within these systems [15].

	Present Limit on $\lvert d \rvert$ $[10^{-27}\,\mathrm{e}\cdot\mathrm{cm}]$	Standard Model Prediction $[10^{-27}\,\mathrm{e}\cdot\mathrm{cm}]$	New Physics Limits $[10^{-27}\,\mathrm{e}\cdot\mathrm{cm}]$
e	$1.8\,(1.2)\,(1.0)$	$\lesssim 10^{-11}$	$\lesssim 1$
μ	$< 1.05\cdot 10^{9}$ (95% C.L.)	$\lesssim 10^{-8}$	$\lesssim 200 \times (\frac{m_\mu}{m_e})^x$
τ	$< 3.1\cdot 10^{11}$ (95% C.L.)	$\lesssim 10^{-7}$	$\lesssim 1700 \times (\frac{m_\tau}{m_e})^x$
p	$-3.7\,(6.3)\cdot 10^{4}$	$\sim 10^{-4}$	$\lesssim 60$
n	$< 63\cdot 10^{0}$ (90% C.L.)	$\sim 10^{-4}$	$\lesssim 60$

Table 1: Limits on Electric Dipole Moments d for electrons (e) [18], muons (μ) [19], tauons (τ) [20], protons (p) [21] and neutrons (n) [22]. For various speculative models the scaling with the lepton mass is stronger than linear (x>0). The number in the first parenthesis for the electron case refers to the statistical error and the second to the systematic.

The upper bound extracted from electron and neutron experiments already disfavor super-symmetric models with CP violating phases of order unity and suggest variants with phases of order α/π [16, 17]. Other significant restrictions of the parameter space would also be an option, however at a loss of generality. A muon EDM experiment at $10^{-24}\,\mathrm{e}\cdot\mathrm{cm}$ will be competitive here. Moreover, it will provide valuable complementary information, because the muon belongs to the second generation of particles where in the quark sector CP violation occurs. In two Higgs doublet models [6] with large ratios for the vacuum expectation values of the involved Higgs fields ($\tan\beta$ ($\leq$ 15)) and for left right symmetry a muon EDM could be as large as a few $10^{-24}\,\mathrm{e}\cdot\mathrm{cm}$ [5] and some special models allow values up to $10^{-21}\,\mathrm{e}\cdot\mathrm{cm}$ [5].

Sensitive searches are presently being carried out on neutral objects, i.e. neutrons, atoms and molecules. This choice was strongly influenced by the Ramsey-Purcell-Schiff theorem [23] which states that for point-like charged objects in electromagnetic equilibrium the net electric field averages to zero. The widely known loopholes so far were

weak and strong nuclear forces, weak electron-nucleon forces and relativistic forces. It is recognized now that this theorem is also not applicable to particles in a storage ring, particularly to the method proposed here, where motional fields are employed, because it is not possible to factorize particle velocity and electric field, which constituted the basis of the theorem [24, 23]. Therefore these electric fields, which are very strong for relativistic particles, can be beneficially exploited. Such fields can be three orders of magnitude higher than technically achievable fields between electrodes, where 5.5 MV/m are regarded an upper limit.

Quantum mechanics requires that there be only one vector possible in any fundamental particle, e.g. its angular momentum $\vec{J}$ [25]. Hence all vectorial quantities must be proportional to this single vector. The magnetic moment $\vec{\mu}$ of a particle is defined as

$$\vec{\mu} = g \cdot \mu_X \cdot \vec{J} \quad , \tag{1}$$

with the magnetic g-factor and the magneton corresponding to the species X of mass m_X

$$\mu_X = \frac{q\hbar}{2m_X} \quad . \tag{2}$$

Permanent EDMs can be defined in a similar fashion

$$\vec{d} = \eta \cdot c^{-1} \cdot \mu_X \cdot \vec{J} \quad , \tag{3}$$

where η in analogy to the magnetic g-factor carries the "interesting physics". For various theoretical models η can be proportional to $m_X^2, m_X^3, m_X^4 ....$ The remaining factors of equation 3 multiply to $9.7 \cdot 10^{-12}$ e $\cdot$ cm for electrons, $4.7 \cdot 10^{-14}$ e $\cdot$ cm for muons, and $5.3 \cdot 10^{-15}$ e $\cdot$ cm for nucleons. In order to compare the physics relevance of the absolute d values, the spins and masses of the particles need to be taken into account.

In the general field of EDM searches, progress in sensitivity can be expected from several approaches. In particular,

- a beam experiment at Berkeley on atomic Tl [18] expects to announce a new result for an electron EDM very soon.

- an experiment on trapped ultra-cold neutrons at ILL has very recently reported a new upper limit on the neutron EDM [22]. Technical improvements are expected to gain half an order of magnitude. Neutron flux is expected to be a severe limitation. Approaches using He-3 as a magnetometer are under way.

- a new technique is expected to yield significant progress for ultra-cold neutrons which are introduced into super-fluid He at temperatures below 1K. Here He-3 is chosen as a co-magnetometer. This experiment is presently performing technical feasibility studies at Los Alamos [25].

- a Hg atom experiment at U. of Washington [26] expects to yield an order of magnitude improvement which includes a higher sensitivity to nuclear EDMs.

- experiments on YbF in Sussex and on PbO at Yale promise significant improvement [27]. In this case an enhancement factor arises from the internal fields in the polar molecules.

- Atoms and molecules in solid He [29] and laser trapped molecules [30].

It has been recognized that the method proposed here is also applicable to searches for permanent EDMs of nuclei [31], provided the system under observation has a suitable magnetic anomaly. Searches for a nuclear EDM would be complementary and competitive, with neutron EDM searches. For heavy nuclei one could expect a quite typical enhancement over a nucleon effect by some factor of 60 due to CP-odd nuclear forces. The feasibility of a nuclear EDM experiment is presently being explored at GSI in Darmstadt, Germany. Experience gained from the BNL muon EDM experiment in controlling the systematics will be very valuable for that project.

For a sensitivity at a level of $10^{-24}\,\mathrm{e}\cdot\mathrm{cm}$, the proposed muon experiment is comparable with present limits on the electron EDM, if the size of the effect is assumed to be inversely proportional to the particle mass. Apparently, the experiment is of special interest for theories where the EDM scales faster than linear by the inverse particle mass [3].

It should be mentioned that the muon is the only second generation particle for which a precision EDM experiment is feasible [32]. Since CP violation is associated with the

second and third generation of quarks only, the muon may have a unique window for new physics in the lepton sector. Therefore, even if there were an EDM observed in another system, a measurement on the muon would be extremely important to understand the nature of the effect [33].

The Muon g-2 Experiment, E821, now being conducted at BNL, has been designed to probe physics beyond the standard model. This includes super-symmetry with large $\tan\beta$ [34, 35, 36, 37, 38] where the muon EDM also has sensitivity. The experiments complement each other, because the magnetic anomaly and the EDM are related to each other as real and imaginary parts of the same physical quantity [39]. The recent new limit on the muon magnetic anomaly [40] corresponds (scaling by e/m_μ) to a dipole moment of order $5 \times 10^{-22}\,\mathrm{e \cdot cm}$ [41], which is well within the reach of this experiment, and demonstrates, how the explored parameter space can be expanded.

4 Experimental Overview

The muon spin precession angular frequency (relative to the momentum vector) in the presence of both electric and magnetic fields is given by

$$\begin{aligned}\vec{\omega} &= -\frac{e}{m}\{a\vec{B} - \frac{a\gamma}{1+\gamma}(\vec{\beta}\cdot\vec{B})\vec{\beta} + (\frac{1}{\gamma^2-1} - a)\frac{\vec{\beta}\times\vec{E}}{c} + \\ &\quad \frac{\eta}{2}[\frac{\vec{E}}{c} + \vec{\beta}\times\vec{B}] - \frac{\eta\gamma}{2(\gamma+1)c}(\vec{\beta}\cdot\vec{E})\vec{\beta}\},\end{aligned} \tag{4}$$

where $a = (g-2)/2$ and η is the EDM in units of $\frac{e\hbar}{4mc}$. This simplifies to

$$\vec{\omega} = -\frac{e}{m}\{a\vec{B} + (\frac{1}{\gamma^2-1} - a)\frac{\vec{\beta}\times\vec{E}}{c} + \frac{\eta}{2}(\frac{\vec{E}}{c} + \vec{\beta}\times\vec{B})\}, \tag{5}$$

assuming the muon velocity is orthogonal to the external magnetic and electric fields ($\vec{\beta}\cdot\vec{B} = \vec{\beta}\cdot\vec{E} = 0$). η plays a role for the EDM corresponding to the g factor for the magnetic dipole moment. The muon EDM couples to the external magnetic field because

in the muon rest frame it looks like an electric field due to the Lorentz transformation. The EDM value in MKS units is given by

$$d_\mu = \frac{\eta}{2}\frac{e\hbar}{2mc} \simeq \eta \times 4.7 \times 10^{-14}\,\mathrm{e}\cdot\mathrm{cm}. \tag{6}$$

From the above equation (5) is apparent why the present $g-2$ experiment uses muons at the "magic" γ, i.e. $\gamma = 29.3$ since at this value the coefficient

$$\frac{1}{\gamma^2 - 1} - a = 0, \tag{7}$$

and the muon spin precession becomes independent of the electric field present in the lab frame. For the dedicated EDM experiment we propose to use muons with much lower energy as well as a radial electric field which cancels the g-2 precession leaving the EDM precession to operate on its own and accumulate over many microseconds. It should be noted that the main component which causes the spin to precess vertically in the muon rest frame is the lab dipole magnetic field which is partially transformed into a radial electric field in the muon rest frame. The electric field in the lab required to cancel the g-2 precession is

$$E = \frac{aBc(\gamma^2 - 1)}{\beta} = 2\,\mathrm{MV/m}, \tag{8}$$

for $\gamma = 5$, $B = 0.24\,\mathrm{T}$ and a magnet radius of 711 cm. Concentric cylindrical plates 10 cm apart with ± 100 KV voltage will satisfy this condition.

Due to the weak interaction decay of the muon to an electron, a muon neutrino and an electron anti-neutrino, the electron angular distribution in the muon rest frame is given by:

$$dP(y,\theta) = n(y)[1 + A(y)\,\cos\theta]dy\,d\Omega, \tag{9}$$

with $y = p_e/(P_e)_{\max}$, the distribution function $n(y) = 2y^2(3-2y)$ and the asymmetry $A(y) = (2y-1)/(3-2y)$. $d\Omega$ is the solid angle element, and θ the angle between the electron momentum and the muon spin. The number of detected electrons above an energy threshold in the lab frame thus probes the angular distribution of the decay electrons in the muon rest frame [42]. The oscillation frequency in the number of detected

electrons is given by equation (5) when the detectors are placed on the inside of the muon storage region [28]. The detector position and the energy threshold in the g-2 experiment is optimized by maximizing NA_L^2, where N is the number of the detected electrons and A_L is the amplitude of the average vector asymmetry given by

$$\vec{A_L} = \int A(y)\, \hat{e}\, dy\, d\Omega, \tag{10}$$

where $\hat{e}$ is the unit vector along the electron direction in the muon rest frame.

From equation (5) (at the muon "magic" momentum) it is apparent that the EDM influence on the spin precession is two-fold: 1) The spin precesses about an axis which is not exactly parallel to the magnetic field but is at an angle $\delta = \tan^{-1} \frac{\eta\beta}{2a}$. The maximum excursion of the muon spin from the horizontal plane, due to an EDM, occurs when the spin is at 90° with respect to the momentum vector. When the spin and momentum vectors are aligned there is no excursion from the horizontal plane. 2) The spin precession frequency is increased by a factor of $\sqrt{(1+\delta^2)}$.

Both of the above methods were used in the last CERN muon g-2 experiment to set a limit on the EDM [19]. They searched for an up down asymmetry in the counting rate with a detector split on the vertical mid-plane. The presence of an EDM induces a difference between the counting rate of the two parts of the split detector at the anomalous spin precession frequency. The reported limit is $3.7 \pm 3.4 \times 10^{-19}\,\mathrm{e \cdot cm}$. The error is the combined result of the statistical and systematic errors:

- Statistical: $\pm 2.7 \times 10^{-19}\,\mathrm{e \cdot cm}$
- Systematic: $\pm 2 \times 10^{-19}\,\mathrm{e \cdot cm}$

Both errors are at the same level. There are at least two sources of systematic errors when the spin is allowed to precess: 1) The center of the muon population is not exactly aligned with the geometric center of the detectors which results to an up-down modulation of the average decay positron position with the g-2 frequency. 2) As the muon spin precesses the decay positrons travel through different magnetic and electric fields before they reach the detector and results again in an up-down modulation of the average decay positron position with the g-2 frequency.

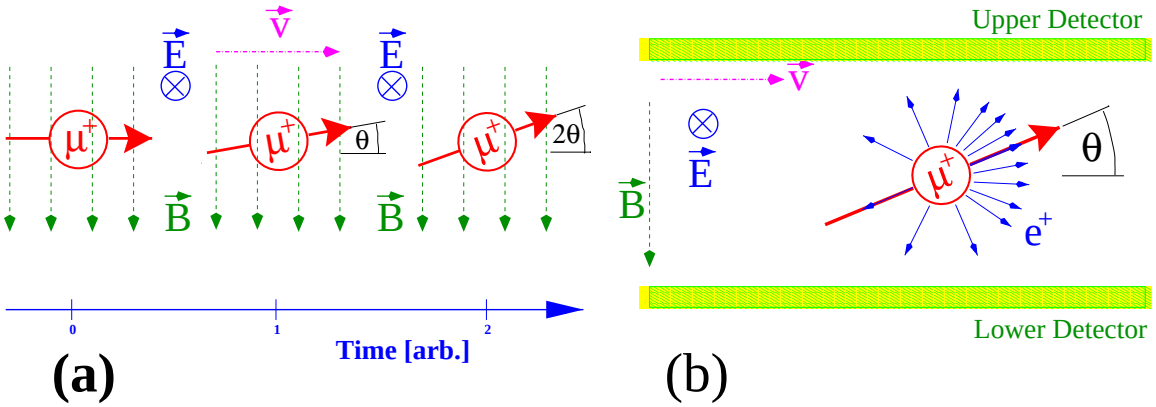

Figure 1: The basic principle of the proposed experiment. (a) Relativistic muons (μ^+) of velocity $\vec{v}$ moving in a magnetic storage ring with field ($\vec{B}$) find themselves exposed to a motional electric field $\vec{E} \propto \vec{v} \times \vec{B}$. In case of a finite small EDM the muon spin precesses with a linear increase in precession angle θ in time about an axis which is directed radially. (b) Due to the spatial anisotropy in the decay $\mu \rightarrow e^+ + \nu_e + \overline{\nu_\mu}$ detectors above and below the storage region are expected to observe a time dependent change in the ratio of positron counting signals. The positron angular distribution is indicated by the density of arrows.

We propose to use a radial electric field to cancel the $g-2$ precession. This together with other improvements will significantly reduce many systematic errors and improve the experimental sensitivity to a muon EDM. The muon spin direction will be "frozen" relative to the muon spin if the EDM is zero. In the presence of a non-zero EDM, the proposed radial E-field (i.e. the motional E-field in the muon rest frame due to the lab dipole B-field) will rotate the spin around an axis parallel to the E-field, thereby tipping the spin vertically. This results in an up-down asymmetry in the number of electrons which is growing linearly with time and this is the quantity which we will measure (see Fig. 1).

Other changes from the present $g-2$ experiment include:

1. Use *magnetic* focusing instead of electrostatic focusing as is used in the present g-2 ring. A 10 by 10 cm area is available for muon storage which will increase the number of stored muons substantially.

2. Eliminate all vertical electric fields from the system during normal data taking. Any

radial magnetic field in the presence of compensating vertical electric field introduces a systematic limitation [46, 47]. For example, in the g-2 ring, a net radial magnetic field of 10 ppm of the main field would produce a systematic error in the EDM of 1×10^{-21} e $\cdot$ cm. A vertical electric field can be used, as discussed later in this note, to calibrate the system sensitivity with high accuracy.

4.1 Target and Beam Line

A preliminary design of an upgraded beam to deliver a high intensity 0.5 GeV/c beam into the acceptance of the inflector of the g-2 ring has been completed. A 10 cm diameter lithium lens 25 cm long transforms the trajectories of 0.9 GeV/c pions produced within an 8 degree cone into a parallel beam matched to the apertures of a pair of 4Q16 quadrupoles. This is accomplished with a field of 0.35 T/cm.

Following the momentum analysis section, a strong focusing channel consisting of 35 4Q24 quadrupoles captures 0.57 GeV/c muons emitted backwards in the pion center of mass system. Pions and muons then enter a second dispersive section in which low momentum muons are separated from the remaining 0.9 GeV/c pions and finally a matching section directs a nearly parallel beam of 0.57 GeV/c muons through a 7.5 cm diameter inflector.

The design upgrade requires the installation of 17 additional 4Q24 quadrupole magnets in the pion decay region in order to capture more muons into the beam channel and 2 new quadrupole magnets in the matching section.

The resulting muon flux estimates were obtained from the Sanford-Wang parameterization [43] of pion production at higher momenta which is incorporated in the beam program BETRAF along with the decay kinematics [44]. The comparison of the estimates for the present g-2 beam and the EDM beam upgrade follows.

	g-2 BEAM	EDM BEAM
	3.1 GeV/c π^+	0.91 GeV/c π^+
π^+/incident proton	2.5×10^{-5}	9.8×10^{-6}
μ^+/incident proton	1.0×10^{-7}	2.4×10^{-7}

The estimate of the pion flux for g-2 pion injection was $2.5 \times 10^{-5}\pi^+$ per incident proton. At 4×10^{13} protons per AGS cycle, this gives $10^9\pi^+$ per AGS cycle. The published result for pion injection [10] gave $10^8\pi^+$/bunch for 4×10^{13} incident protons in 8 bunches to give $8 \times 10^8\pi^+$ per AGS cycle.

With an anticipated AGS flux of 10^{14} protons per cycle, this implies a $1.2 \times 10^7\mu^+$ per AGS cycle assuming a 50% storage efficiency allowing the accumulation of 10^{14} stored muons in approximately 4000 hours.

Incremental increases in flux could be obtained through refinements in the design. For example, the lithium lens position could be moved closer to the production target and the inflector aperture might be increased. Available data at low pion momenta indicate at least a factor of two over what is predicted by Sanford-Wang and we are currently investigating them. We are also investigating the possibility to use a magnetic horn instead of the Li lens and are comparing the pion collection efficiency and the hardware requirements between the two choices.

4.2 Weak Focusing Ring

The weak focusing magnetic field index is:

$$n = \frac{R_0}{B_0}\frac{dB_r}{dy} \tag{11}$$

The accepted emittances and dp/p are:

$$\epsilon_V = A_V^2 \frac{\pi\sqrt{n}}{R}$$

$$\epsilon_H = A_H^2 \frac{\pi\sqrt{1-n}}{R}$$

$$\frac{dp}{p} = \frac{(1-n)A_H}{R}$$

For the g-2 experiment, a circular aperture with 45mm radius was used. Inside this radius, the magnetic field was uniform to about ±1 ppm. Obviously, this is over-kill for the edm experiment, and the aperture should be at least ±50 mm square. This gains a factor of 3 in acceptance.

The inflector magnet used for the g-2 experiment had an aperture of 18mm (H) by 56mm (V) and a length of 1.7m. The limited aperture was due to the technical difficulty of canceling the 1.45T field. The measured transmission was 72%. By increasing the aperture, we anticipate increasing the transmission to 1.0. Also, the beam passed through about 0.1 radiation lengths of material. With a normal magnet canceling the 0.23T field, the beam can simply pass through in vacuum. The multiple scattering in the 0.1 radiation length of material was estimated to reduce the storage efficiency to 57% compared to an open design. The muon beam then passed through the outer Q1 electrode. This further reduced the storage efficiency to 80% compared with an open design. It is possible in the EDM experiment to eliminate this loss if the outer dipole electric field electrode is at a larger radius than the injected beam. In the g-2 experiment, the kicker high voltage was low by about 10% resulting in about 20% loss of storage efficiency. The required HV is much less for the edm experiment.

The g-2 experiment accepted emittances are given below:

g-2	H (π mm mrad)	V (π mm mrad)
Beamline	42	56
Inflector	53	64
Storage Ring	168	66

We have not decided upon a field index for the EDM experiment. Taking the g-2 experiment n = 0.137 gives for the EDM experiment:

EDM	H (π mm mrad)	V (π mm mrad)
Beamline	≈ 150	≈ 150
Inflector (6 cm H by 10 cm V)	177	125
Storage Ring (10 cm H by 10 cm V)	264	125

We do not fill the storage ring horizontal emittance. However, we don't want to reduce AH, because then we would reduce the dp/p acceptance. The dp/p acceptance is $\pm 0.6\%$ for weak focusing, whereas it was six times larger for the strong focusing study in the 1997 LOI. It is therefore estimated that the number of muons stored will be by roughly a factor of 10 less than with strong focusing.

4.3 Inflector

The injection of beam into the storage ring is usually done with a septum magnet (inflector), which locally cancels the field of the main magnet, so that the beam enters the storage region nearly tangential to the equilibrium orbit.

A direct current non-ferrous super-conducting inflector has been designed and constructed for E821 (muon g-2) [28]. Double cosine function related current density is applied on an arc with a radius of 5 cm. Truncation is carried out along one of the constant vector potential lines, by placing conductors corresponding to certain current density [45]. The dipole field is uniform in the beam channel and there is very low fringe field in the vicinity of the device. E821 required 2850 A current in 88 turns to provide a 1.5 T channel field. For the muon EDM experiment, only one sixth of the current is required.

In the EDM experiment the leakage field requirement is much more relaxed and simpler designs are acceptable. We are planning to use a water cooled normal conductor with the geometry shown in Fig. 2 The figure shows the cross section of the inflector (the two parallel plates with the enclosed flux) and the $g-2$ magnet with the pole pieces as shaped currently. Fig. 3 shows the magnetic flux when both the main magnet and the inflector are powered. Fig. 4 shows the vertical component of the magnetic field in gauss over the storage region (from 706.7 to 715.7 cm) with both the inflector on and off. The influence of the inflector at the muon storage area can be further reduced by shimming it to the

required accuracy.

4.4 Storage Ring-Weak Magnetic Focusing

The g-2 ring magnet has been built to provide excellent field stability and homogeneity for precision measurements. For the EDM experiment the field homogeneity is of relatively little concern, but the stability of the magnetic field, specifically it's direction, is extremely critical. Measurements of the minor field components were done with Hall probes to an accuracy of about 10 ppm. During data taking runs the maximum number of muons is stored if the beam is vertically centered with respect to the electrostatic quadrupoles. Current coils on the pole faces are used to compensate the static radial field average. From these measurements we know that the average radial field $< B_r >$ changes by 20 ± 10 ppm year to year.

For the EDM experiment we aim to improve our knowledge of $< B_r >$ by three orders of magnitude. From the NMR measurements of the absolute field we know that the variations in the magnetic field are dominated by changes in the vertical gap between the upper and lower pole pieces due to thermal expansion/contraction of the magnet steel including the super-bolts that hold the yoke pieces together. A uniform temperature rise leads to an increase of the air gap and thus a reduction of the magnetic field in the storage region but does not change the direction of the field. However, the thermal time constant of the yoke is several hours, and changes in the ambient temperature do not only change the average vertical gap but also cause a transient relative tilt of the top pole with respect to the bottom. This affects the direction of the magnetic field, introducing a small radial field component, as well as the normal quadrupole moment, i.e. the gradient of the vertical field along the radial direction. In a weak focusing magnet we can use NMR probes to keep track of the radial field change by precisely measuring the normal quadrupole moment. These measurements should be compared to direct measurements of the gap variation using optical interferometry. During the first g-2 run in 1997 data were taken in a constant current mode and the ambient temperature changes are clearly visible in the average field, see Fig. 5. Fig. 6 shows the change of the normal quadrupole moment in the same time period. This change is highly correlated with the temperature difference

between the magnet yoke surface temperature and the ambient temperature, also shown in Fig. 6. Since 1997 the magnet yoke has been insulated and the temperature effects are reduced by about an order of magnitude, see Fig. 7, but the radial field component could still change by a few hundred nanoradians over a day. Even with further improvements in the temperature stability, this change will have to be monitored and compensated, e.g. with the existing pole surface current coils.

Most of the pulsed NMR equipment for g-2 could be used in the EDM experiment. Only the passive probes and the pulse amplifiers have a narrow bandwidth and would have to be redone.

In order to measure the average field component in the E-field direction with a deuteron beam, either the E-field or the B-field will have to be changed. In both cases the dependence of the field direction on the field strength is a concern. For the B-field there is a strong dependence due to the attractive magnetic force. At the g-2 field of 1.45 Tesla the average gap is reduced by 0.3 mm relative to the zero field value and the top pole rotates by about 0.3 mrad with respect to the bottom pole during the ramp. This translates into a tilt change of about 1.0 μrad or a change in the radial field component in the mid-plane by 0.5 ppm while going from 0.218 T (deuteron) to 0.233 T (muon). Again this change can be monitored accurately with NMR probes and also with optical interferometers. Using both methods would give additional information on field perturbations due to permeability changes which are expected to be small at these low field values.

4.5 Storage Ring-Strong Magnetic Focusing

Since the search for an EDM does not require an accurately known magnetic field, the use of strong magnetic focusing is very advantageous. We plan to use the 36 pole pieces on top and 36 on bottom shaped in such a way that they provide $\frac{\partial B}{\partial R} = 1.45$ T/m of 36 alternating gradient focusing regions. The main dipole field (for the 0.5 GeV/c muon momentum case) is 0.24 T and therefore the regional field focusing index is $n = 43$. The phase advancement is 44.5° per region. Assuming the same muon storage region of 9 cm in diameter, as in the current g-2 experiment, the estimated beta functions are $\beta^x_{max} = 4.5$ m, $\beta^y_{max} = 4.3$ m. The compactification factor is 5.9 giving an overall

factor of 50 improvement in the number of stored muons over a comparable system with an electrostatic weak focusing. We are also considering a redesign of the beam storage vacuum chamber to optimize it for the EDM experiment.

There is a need to have a kicker in order to be able to inject muons into the ring. One third in length of the current kicker with two thirds the peak current would suffice. The eddy currents of this kicker would be sufficiently low not to become a source of systematic errors.

4.6 Storage Ring Lattice

There need to be azimuthal gaps in the dipole electric field electrodes for the inflector, kicker, pickup electrodes, and deuteron spin analyzer. Therefore, we have chosen four-fold symmetry for the lattice. At this time, 1 m gaps seem to be adequate. A Fourier analysis $F(s/R) = \sum A_N \cos(N_s/R)$ gives the results indicated in table 3:

Table 2: Fourier Coefficients of the Ring Lattice

N	%	N	%	N	%
0	91.1	28	-4.2	56	1.7
4	-8.8	32	-3.1	60	1.4
8	-8.5	36	-2.1	64	1.9
12	-7.9	40	-1.1	68	1.9
16	-7.2	44	-0.2	72	1.7
20	-6.3	48	0.6	76	1.4
24	-5.3	52	1.2	80	1.0

The effect on the equilibrium orbit is given by:

$$dx_e = RE_N \frac{\cos(N_s/R)}{(Bv - E)(-N^2 + 1 - n)} \tag{12}$$

for the deuteron, and change the sign of E for the muon. We have not yet chosen the weak focusing field index n:

$$n = \frac{R}{(B_0 - E_0/v)} \frac{\partial(B_y - E_x/v)}{\partial R} \tag{13}$$

For n=0.137 (the current muon g-2 weak focusing field index) the effect is about ±1cm for the deuteron and ±1.7mm for the muon. The aperture will be defined by the electric dipole electrodes of ±5cm vertically and horizontally. This dx_e is acceptable, and could be further minimized by adjusting the electrode High Voltage as a function of azimuth.

For E821 the muons passed through the outer quadrupole #1 electrodes and insulators at x = 5cm between the exit of the inflector magnet and the kicker. The Coulomb multiple scattering in quadrupole #1 reduced the muon storage efficiency by about 20%. For the EDM experiment, the outer electric dipole electrode between the inflector and the kicker will be at larger radius than the inflector aperture, eliminating this loss of storage efficiency. With the new inflector magnet design where the beam passes through a significantly larger aperture in vacuum, the E821 loss of muon storage efficiency of a factor of two will also be eliminated.

4.7 Detectors

We require a detector system which is sensitive to the number of muon decay electrons going upward compared to the number going downward, in an energy range of 100 to 500 MeV. The up-down asymmetry, $\frac{N_{up}-N_{dn}}{N_{up}+N_{dn}}$, is directly proportional to η and the EDM. The detector should be relatively insensitive to background from muons, neutrons, pions, protons, etc.

The detectors will also have to be capable of handling the extremely high instantaneous rates immediately following muon injection, and the efficiency for measuring the up-down asymmetry must remain stable when the rate diminishes as the muons decay.

We anticipate that 10^7 muons will be stored per AGS bunch, significantly more than, for example, what the muon g-2 experiment currently receives. There will be 12 bunches, separated by about $33ms$, as in the g-2 experiment. The muons have momenta of 500 MeV/c, $\gamma = 4.83$, and mean lifetime=$10.6\mu s$. The average time spacing between muon decays is then $10.6 \times 10^{-6}s/10^7 \approx 10^{-12}s$. If we assume that we have approximately 1000-fold segmentation in the detector system, then each counter would have an average

event spacing of $1ns$ immediately after injection. At ten lifetimes, the average spacing between events increases to $22.0\mu s$. Thus, the detector must be capable of measuring the number of electrons over a large dynamic range of rates and for a large initial rate.

Individual electron counting is impractical at early times because the time spacing between events is too small. Consequently, we plan to integrate the total charge from the detectors. This implies that the gains of the detectors must be exceptionally stable. The geometric arrangement of the counters will be up-down symmetric so as to minimize up-down asymmetries arising from backgrounds.

The proposed system consists of 2 cm thick lead-glass slabs placed above and below and on the sides of the storage region, with photodiode readout. The radiation length is about 1.5 cm. The electrons, on average, enter the lead-glass at large angles with respect to the orthogonal plane. Simulations show that the rms energy resolution for 400 MeV electrons is about 14% due to shower fluctuations and losses. Photon statistics will increase this; for regular lead-glass, the resolution will increase to about 25%, less if scintillating lead-glass is used. About 60% of the electrons above 100 MeV fall into the main shower peak, with the rest falling in a low-energy tail. On average, the showering electrons will leave much more energy than, say, muons which are lost from storage or gamma rays from neutron capture, thereby minimizing background sensitivity.

The lead-glass slabs would cover the top and bottom areas of the pole tips, and will go around the 43 m circumference of the ring minus 4 m for the required gaps. Most of the decay electrons will be intercepted by such a geometry, as indicated by the radial distribution of electrons striking the detectors in Fig. 8. It will be segmented in 10 cm sections, each section being read out by a photodiode. This provides an overall segmentation of about 800.

The photodiodes will have time constants of about 1 μs. At the high anticipated rates, individual counting of decay electrons will not be attempted. Instead, we will integrate the total charge accumulated in approximately 1 μs intervals, as a function of time after injection. The charge will be calibrated to the number of decay electrons, and the up-down ratio as a function of time after injection will be deduced.

The measurements will be taken for about ten muon lifetimes after injection, or for

about 110 microseconds, however, most of the data will be collected in the first 55 μs. The gains of the photodiodes must be extremely good over 55 μs: to about 1 part in 10^5. We are working with the Instrumentation group at BNL to develop such an ultra-stable system. Their first analysis indicates that one can stabilize the gains to 1 part in 10^4 and then calibrate the gain to 10%, thus providing the needed 1 part in 10^5 stability.

Given the demanding stability requirements, we are investigating schemes where the effect of any drifting in the photodiodes would cancel. One possibility is to alternate the measurement between muon spins parallel and anti-parallel to the muon momentum; a non-zero EDM would lead to a positive value for $\frac{N_{up}-N_{dn}}{N_{up}+N_{dn}}$ in one case and a negative sign in the other. (This is not a perfect systematic check, however, since one spin direction would have a lower average energy than the other, as seen in Fig. 9).

One possible way to collect data for both parallel and anti-parallel spin orientations would be to alternate between injecting forward and backward muons, which have opposite spins. Unfortunately, even if a way could be developed to quickly switch between the two, the forward muons would probably have an intolerable pion and proton contamination. Another possibility would be to allow the muons to precess naturally in the B-field of the storage ring until their spins are reversed, then switch on the radial E-field to halt the precession. In the proposed B-field at 500 MeV it would take 13.5 μs for the spin to precess 180 degrees, but this could be sped up if the radial E-field which is used to halt the spin is initially reversed. The challenge is to be to able to switch the radial E-field in a sufficiently short time (few microseconds), and also to deal with the change in the muon storage radius as the radial field is changed.

Fig. 10 shows the number of decay electrons vs energy which strike the detector, the up-down asymmetry=$\frac{N_{up}-N_{dn}}{N_{up}+N_{dn}}$, and the relative statistical power of the electron data, which is proportional to the inverse of the relative error on the up-down asymmetry.

5 Sensitivity Level

The EDM sensitivity is given by (in MKS units)

$$\eta = \frac{2\theta_t}{\beta B t}\frac{m}{e}, \tag{14}$$

with θ_t the minimum transverse spin precession angle which can be detected, m, e the muon mass and charge respectively, and B, the average magnetic field seen by the muon. The uncertainty in η is

$$\sigma_\eta = \frac{1}{\gamma \tau_0 A_1 A \sqrt{2N_{Tot}}}, \tag{15}$$

with $A_1 = \beta e B/2m = 10^8/\mathrm{s}$ for $B = 0.24\mathrm{T}$, N_{Tot} the total number of observed decays, τ_0 the muon lifetime at rest, γ the Lorentz boost factor, and A the asymmetry. If one observes 1.5×10^{15} decay electrons which have an average transverse asymmetry of 0.3 then the uncertainty in η is 5.5×10^{-11}, and on the EDM $2.5 \times 10^{-24}\,\mathrm{e \cdot cm}$. In two muon lifetimes (i.e. $2 \times 11\mu\mathrm{s}$) this corresponds to a vertical precession angle of 120 nrad.

The sensitivity of the experiment increases as the B field and the lifetime increase. However, the necessary electric field which is canceling the muon $g-2$ spin precession also grows fast as can be seen by equation (8).

When the ring is working in the strong focusing mode an estimated total number of 10^{14} stored muons in 4000 hours will yield a statistical limit of $10^{-23}\,\mathrm{e \cdot cm}$ is possible. In the weak focusing mode (but with the modified beamline and inflector) the estimated number of muons will be 10 times less and therefore a limit of $10^{-22}\,\mathrm{e \cdot cm}$ is possible in only 400 hours.

If the claimed sensitivities can be accomplished and the experiment is statistics limited then we will apply the techniques pioneered by the muon collider, muon storage ring and the meco collaborations to improve the limits down to $10^{-24}\,\mathrm{e \cdot cm}$ by injecting 100 times more muons.

5.1 Calibration of Sensitivity

A simple way to calibrate the experimental sensitivity to the muon EDM is to apply a vertical electric field in the muon storage region. The beam will be displaced vertically until the magnetic focusing will compensate with an equal and opposite force. The average radial magnetic field seen by the muons will be such that it compensates the vertical

electric field. This non-zero radial magnetic field will induce a non-zero spin precession in the vertical plane mimicking an EDM effect.

The vertical spin precession angle with a vertical electric field E_v, and a vertical B magnetic field present is given by

$$\theta_t = \frac{e}{2m}[g\frac{E_v}{c\beta\gamma^2} + \eta\beta B]t, \tag{16}$$

which for $E_v = 5$ KV/m results in 30 mrad vertical spin precession which is easily measurable. This average electric field can be achieved by placing pulsed 25 KV on a pair of electrodes, 10 cm apart, covering 2% of the ring.

It should be noted that in the absence of an electric field the average radial magnetic field seen by the muons is exactly zero since we are using *magnetic* focusing.

6 Systematic Errors

Potential systematic errors include the following:

1. Early to late electron counting (rate) effects. With almost 10^7 muons entering the ring and a good fraction of them decaying within $10\,\mu s$ the rates are very high. Our detector will be scintillating lead-glass calorimeters with photodiode readout. The readout electronics are specially made so that they maintain their linearity to 10^{-4} [48] and will be measured to 10%. With 800 such systems the error is further reduced another factor of 30. We are investigating the possibility of interchanging electronically the top/bottom detector readout randomly about 100 times which brings us to 3×10^{-8} linearity error in the electronics.

2. Proton or pion contamination of the muon beam. During the 1997 run of the g-2 experiment about 10^8 pions per spill were injected, the pion flash was the biggest problem. After striking a nucleus hadrons produce secondary neutrons which in turn produce gammas paralyzing the photo-multipliers mostly at the first half of the ring for tens of μs. When we tried the muon injection by lowering the accepted particle momentum by about 1.5% the light flash went down by a factor of 50.

In the muon EDM experiment the secondary beam is 900 MeV/c whereas the muons have half that. One can expect a proton/pion leakage of less than 10^{-4} per muon. It is therefore the lost muons (assuming 50% storage efficiency) which will dominate the flash. Their efficiency (μ^+ case) of producing neutrons is down by approximately a factor of $\alpha \approx 1/137$ relative to those produced by pions/protons. We plan to study this effect with the kicker off and observe its time dependence and up/down asymmetry. This effect is still under study.

3. Muon losses as a function of time. If there are muon losses at an appreciable level and get lost in a non-uniform way they could provide a false signal. We are studying the potential level of this effect and ways to minimize it (e.g. scraping, under-filling the vertical and horizontal acceptance of the ring, etc.).

4. Stored positrons. Positrons from the beamline with the same momentum as muons will be stored in the ring and will synchrotron radiate their energy at a rate of 0.8 KeV per revolution. For 0.5% momentum acceptance of the ring, it will take approximately 1 ms before all positrons reach the inner aperture whereas almost all the muons decay within 50 μs. We are studying the potential problems and possible uses of the stored positrons.

5. Due to the cylindrical nature of the electrostatic plates which provide the radial electric field, the E-field decreases as $1/R$ making the cancelation of the g-2 imperfect as a function of the muon momentum. Also, taking into account that the spin precession cancelation depends on both the magnetic field and the value of gamma (see equation (8)), one can estimate that at the edge of the aperture, the muon spins will flip horizontally in 100 μs. Only a very small fraction of the muons will do that. We are investigating the requirement on the acceptance and detector efficiency uniformity so that this effect is also negligible. At any rate this error will be known by letting the muon spin precess and observing the precession plane as a function of the E-field.

6. The problem with radial B-fields when using electrostatic focusing is eliminated completely because we use only magnetic focusing. However the misalignment and

time stability of the E and B-fields is going to be monitored by the inclinometer and the laser interferometers described next.

7. Horizontal and Vertical coupling of the betatron oscillations. Yuri Orlov is studying this effect.

8. The "vertical" component of the E-field, i.e. the average component of the E-field along the B-field should be known to $\pm 10^{-8}$ of E for $1 \times 10^{-24}\,\mathrm{e} \cdot \mathrm{cm}$ limit. This is addressed below.

We feel confident that we can analyze all sources of systematic errors and greatly reduce them due to the flexibility provided by a dedicated muon EDM experiment.

6.1 Electrode alignment

The vertical component of the electrostatic field in the muon storage region, averaged over the ring circumference, must be well suppressed. An average component of 10 nrad will induce an effect mimicking an EDM of $10^{-24}\,\mathrm{e} \cdot \mathrm{cm}$. This implies that the electrodes, and the resistive top and bottom plates used to produce a uniform electrostatic field, must be aligned with respect to the horizontal plane with high precision.

Fig. 11 shows a method that may be used to achieve this alignment and most importantly the monitoring of the relative distance to better than 10 nrad. The electrodes and top and bottom plates are clamped at intervals with pairs of U-shaped machinable ceramic yokes. The top and bottom plates are made of glass doped to produce a small but uniform conductivity bonded to insulating webbing for support. The outer surfaces of the conductive glass are covered with an anti-reflection coating so that the parallelism of the inner surfaces of the top and bottom plates may be tested, after clamping, by optical interferometry. Shimming may be necessary to insure that these inner surfaces are parallel. We are investigating the possibility of constructing the plates of scintillating lead glass to be used as an almost full acceptance detector for the decay positrons. The cross section of the plates (10 cm by 10 cm) is shown on the right. The top and bottom plates consist of conductive glass plates. On the top of the figure the laser interferometer is shown which

has 5 nm relative position resolution and 33 KHz response speed. Integrating over 3 ms will result to 5 nrad angular resolution [49].

6.2 Inclinometer

As discussed above, the difference between the cyclotron and spin precession frequencies is:

$$\vec{\omega} = -\frac{e}{m}[a\vec{B} + (\frac{1}{\gamma^2 - 1} - a)\frac{\vec{\beta} \times \vec{E}}{c} + \frac{\eta}{2}(\frac{\vec{E}}{c} + \vec{\beta} \times \vec{B})] \tag{17}$$

For this experiment, an electric dipole field is generated such that:

$$a\vec{B} + (\frac{1}{\gamma^2 - 1} - a)\frac{\vec{\beta} \times \vec{E}}{c} \approx 0 \tag{18}$$

This requires that over the ensemble of particles that $\vec{B} \cdot \vec{E} \approx 0$ and

$$E \approx aBcp(1 + \frac{p^2}{m^2})^{1/2}/m \tag{19}$$

This equation is a useful approximation for the following discussion. It would be useful to find a particle which can be stored in much greater (polarized) numbers than the muon, and which has a similar factor:

$$F = a(1 + \frac{p^2}{m^2})^{1/2}/m \tag{20}$$

In table 3 we give the factor F for the muon, proton and deuteron for E = 2MV/m and R=7.11m.

Table 3: The factor F for different particles

Particle	a	$(1 + p^2/m^2)^{1/2}$	m (MeV/c^2)	F
μ	0.001166	≈ 5	105	0.054
p	1.793	≈ 1	938	1.912
d	-0.143	≈ 1	1876	-0.076

The deuteron has F close to the muon in magnitude. In table 4 we show the momentum p, the velocity β, the γ factor and the required B-field for E=2MV/m, R=7.11m for the muon and deuteron.

Table 4: Muon and deuteron parameters

	μ	d
p (MeV/c)	511.	396.
β	0.979	0.207
γ	4.94	1.022
B (T)	0.233	0.218

For the μ^+, B is directed up and E points toward the center of the ring (beam goes clockwise as seen from above the ring). In units of GeV/c, T, V, and m:

$$p \approx 0.3[B + E/v]R \tag{21}$$

For the deuteron, B is directed up and E points away from the center of the ring.

$$p \approx 0.3[B - E/v]R \tag{22}$$

The amazing coincidence is that although the muon and deuteron a and γ differ by orders of magnitude, the B-field is the same to 0.015T for $\mid E \mid = 2$MV/m and R = 7.11m.

As discussed above, the angle θ between $\vec{B}$ and$\vec{E}$ over the ensemble of particles should be known to 10 nrad for a systematic error on the EDM of the muon at the 10^{-24} e $\cdot$ cm level, since this causes the same spin precession as an EDM:

$$dS/dt = \mu\theta E/(c\beta\gamma^2) \tag{23}$$

For the deuteron, $\mu = 0.857e\hbar/(2m_p)$, and for the muon, $\mu = 1.001e\hbar/(2m_\mu)$. For $\theta E = 10^{-8} \times 2$MV/m, $\omega_s = 14$ mrad/s for the deuteron, and 2.3 mrad/s for the muon. Since the effect is six times greater for the deuteron, the deuteron integration time is much longer, and much larger numbers can be stored, the deuteron is a great system to sense the average direction of the E-field compared to B-field.

The spin precession due to the edm is:

$$d\vec{S}/dt = \vec{d} \times (\vec{E} + \vec{v} \times \vec{B}) \tag{24}$$

The ratio of the sensitivity of the deuteron to θ compared to the edm is 10^2 times larger than for the muon. From the present sensitive limits on the edm of the neutron and Hg, the edm of the deuteron is not a systematic error to using it as an inclinometer for the measurement of the muon edm at the 10^{-24} e $\cdot$ cm level.

6.3 Deuteron Polarimeter

The present AGS polarized proton source could produce polarized deuterons with a polarization of about 75%. A deuteron RFQ would need to be built. This would cost about \$300K. The efficiency for accelerating deuterons would be low, since the AGS complex is optimized for protons. The estimates are 5-20% efficiency for the Linac and about 20% efficiency for the Booster/AGS/Beamlines. This would produce about 5×10^9 deuterons per AGS cycle with an emittance of about 30πmm-mrad. The momentum spread would be about 10^{-3} with a repetition rate of about 5 Hz.

To achieve an error on the measurement of the muon electric dipole moment of 10^{-24} e$\cdot$ cm, the angle between $\vec{B}$ and $\vec{\beta} \times \vec{E}$ from the imposed 2 MV/m electric field must be known to $\delta\theta = \pm 0.01$ μrad $= 10^{-8}$. The deuteron beam for which the in-plane spin precession is canceled (as it will be for the muon) has $\beta = 0.207$ (about 41 MeV) in the same electric field. Errors in the field direction ($\vec{\beta} \times \vec{E}$ pointing at an angle $\delta\theta = 10^{-8}$ away from $\vec{B}$ in the **E-B** plane) will cause the longitudinally polarized deuterons to precess into the vertical direction at a rate of $dS/dt = 14$ mrad/s.

A collimator at 180 degrees in the storage ring will pass particles with dp/p $\sim 10^{-4}$ (about 5×10^8 deuterons). With a momentum spread of 10^{-4} in the stored deuteron beam, it is estimated that a practical upper limit on the observation time for electric field inclination errors is about 5 ms before momentum errors have caused the deuteron polarization direction to spread in angle and effectively de-polarize. In 5 ms, an error of $\delta\theta = 10^{-8}$ has created a precession of 70 μrad. In practice, the 5-ms observation window should be divided into at least three separate measurements (about 1.5 ms each) so that

the slope of the vertical polarization component with time is also apparent. This will help to subtract contributions from any extra vertical components that are present in the beam at injection. Because the cycling of the machine will provide new fills at a rate of only 5 Hz, these measurements inside the observation window will have a duty factor of $< 1\%$.

The deuteron beam is expected to have a polarization of about 75% of the theoretical maximum, a value that depends on the choice of the polarization state of the source. If sufficient flexibility is available, the best states to choose are those with the deuteron spin projection $m = 1$ and $m = -1$, even though they are tensor as well as vector polarized. The spherical tensor value of this vector polarization is $it_{11} = 0.65$. Corrections to the measurement can be made for the effect of the tensor polarization on the cross section and consequently on the measurement of the vertical component of the deuteron polarization in the ring if the properties of the analyzing nuclear reaction are well understood.

The best target for a measurement of the deuteron vector polarization appears to be hydrogen. At 41 MeV, the vector analyzing power is largest ($iT_{11} < -0.15$) in the range $\theta_{c.m.} = 84°$ to $121°$ [50, 52]. The scattered deuterons emerge between 18° and 27° in the lab, and the recoil protons appear between 41° and 60°. Both particles should be detected, along with their relative time of flight. This has proven crucial in separating the background from deuteron breakup [51] in other observations of p+d elastic scattering. If pulse height and time cuts are to be imposed in the electronics, then the detectors will need to be segmented in angle to allow for changes in the elastic scattering kinematics.

The vertical component of the vector polarization creates a left/right asymmetry in the cross section. Two pairs of coincident detectors operating in the angular ranges stated above will be used to observe this shift. These detectors can also span 90° in azimuth with a loss of analyzing power of only 10%. The average analyzing power integrated over this detector acceptance is $\langle iT_{11} \rangle = -0.22$. This leads to an asymmetry for the full beam polarization of $\epsilon = 2iT_{11}it_{11} = -0.26$.

The number of events needed to make an asymmetry measurement to a level of precision δ_1 (the one standard deviation error on the asymmetry ϵ) is $C = 1/\delta_1^2$ (for $\epsilon \ll 1$). The vertical component of the polarization must be measured to a fractional error of

7×10^{-5}, as noted earlier. So $\delta_1 = (7 \times 10^{-5})|\epsilon| = 1.8 \times 10^{-5}$. This requires 3×10^9 events for each data point.

Several target options are under consideration. The first would be to introduce the hydrogen as a gas jet with a gas catcher and two or three stages of differential pumping mounted from the inside of the g–2 ring. Given a nominal beam from a polarized ion source and a new RFQ acceleration channel, present acceleration and beam transport efficiencies would suggest that 5×10^8 deuterons with dp/p $\sim 10^{-4}$ could be stored in the ring with each fill. At $\beta = 0.207$, the revolution frequency of the beam is 1.3 MHz, resulting in a circulating current of 0.1 mA (7×10^{14} s^{-1}). While gas jet targets have operated at densities as high as 10^{16} cm^{-2}, a working thickness is typically 3×10^{15} cm^{-2}. This produces a luminosity of 2×10^{30} cm^{-2}s^{-1}.

The d+p elastic scattering cross section integrated over the detector acceptance described earlier is roughly 8.4 mb. The product of this with the luminosity and duty factors given above would produce about 130 events/s. The instantaneous rates during the brief data accumulation windows would be close to 2×10^4 s^{-1}. To measure the systematic uncertainty in the positioning of the electric field to the required accuracy at this rate would require roughly half a year of running. Thus it would be important to strive for much larger luminosities should this be the preferable targeting method.

A second target option is to use fibers or ribbons of solid CH_2 that would intercept the beam. This option has much greater effective density than the gas target. Self-supporting targets can be made. A thin gold layer on either side has proven helpful in conducting away the heat from interactions with the beam [51]. In order for energy loss of the reaction products in the target not to become an issue, the target would have to be less than 20 mg/cm^2 thick to the beam. A thin ribbon placed in the middle of the beam could serve as a target, but it would be essential to investigate in detail whether a target of a hydrogenous material could survive the heating from the beam. (Targets of a thin ribbon of carbon have greater resistance to the effect of beam heating, but do not have useful analyzing powers for reaction products going in the forward direction.) Another approach is to place the target at the edge of the beam and perhaps move it toward the beam center as the measurement proceeds. This has the disadvantage that the source of

reaction products is not necessarily centered with respect to the detectors and systematic errors in the asymmetry measurement would be harder to control.

Regardless of the targeting scheme or luminosity, there are other limits to the rate of data acquisition. So long as individual particle counting is required in order to identify deuterons and protons from d+p elastic scattering, instantaneous rates will need to remain below 10^6 s^{-1}. With the duty factor of 1%, the real rate is closer to 10^4 s^{-1}. At this rate, 3 or 4 days of data accumulation are required to reach the goal of 3×10^9 events. Data acquisition schemes that involve integrating the particle flux from many events at once would have to investigate the spin dependence associated with protons from deuteron breakup and how these would be recorded in any particular detector arrangement given the spread of energies and angles from three-body phase space.

For asymmetry errors of the order of 2×10^{-5}, systematic errors in the measurement will need to be suppressed. This is typically done through comparing measurements made with both positive and negative polarizations of the beam, and with detectors on both sides of the beam. Then if the asymmetry is calculated using left (L) and right (R) count rates from

$$\epsilon = \frac{r-1}{r+1} \qquad r^2 = \frac{L_+ R_-}{L_- R_+}$$

the systematic errors are proportional to the asymmetry and therefore small. Additional precautions involving the symmetric location of the target and beam would need to be incorporated and studied so that their influence on the results would be understood.

It is our goal to be able to make the deuteron measurement in four hundred hours of beam-time (four weeks at one hundred hours per week) including detector checkout and systematic studies. Then the AGS would be switched from polarized deuterons to high intensity protons (several weeks). The muon measurement would be made in one thousand hours of beam-time, including detector shake-down and systematic studies. The stability of the electric and magnetic systems would be tracked over this period with the systems described above.

6.4 Pickup Electrode Measurement of Vertical Component of Electric Field

The AGS can deliver about 5×10^9 polarized deuterons with $dp/p = 10^{-3}$ and emittance about 30π mm – mrad at 0.4 GeV/c momentum. The average vertical position of the beam will be where:

$$\vec{F} = q(\vec{E} + \vec{v} \times \vec{B}) = 0 \tag{25}$$

Of course, there will be betatron oscillations about the average. For a weak focusing machine

$$n = \frac{R_0}{B_0}\frac{dB_r}{dy} \tag{26}$$

The change in height due to the vertical electric field will be:

$$dy = \frac{R_0}{B_0}\frac{E_v}{vn}$$

We haven't yet decided on an n value for the edm experiment, however, for discussion purposes, let's take n = 0.137 (this is what the muon g-2 experiment used). For weak focusing, the accepted emittances and dp/p are given above in the Weak Focusing Ring subsection.

The deuteron betatron oscillations would occupy ±24 mm vertically, and ±15 mm radially (for dp/p=0). dp/p = 10-3 would occupy ±8 mm (equilibrium orbits). Then $dy = 0.1\,\mu$m, for B = 0.2T, R = 7.11m, and $E_v = 10^{-8} \times 2$MV/m. This is very small; however, we would be measuring differences. This could be measured with pickup electrodes (described below) or by kicking the beam onto a detector. By kicking the beam onto a segmented detector, we would have a sensitivity of $24\text{mm}/\sqrt{N}$ or $0.1\,\mu$m per AGS pulse. Also, we will run with positive and negative E, i.e. pointing inward and outward.

The beam position monitor (BPM) for the deuteron beam vertical shift, due to a vertical component of the electric field consists of four 1 meter long pickup electrodes, installed symmetrically around the beam. The electrodes are connected to ground potential through variable capacitors needed for electrically zero tuning of the monitor. The

induced voltage is q/C_i, where $C_i = C(\text{variable}) + C_0$ where C_0 is the capacitance of the electrode. $q \approx Ql/L$ with l the monitor length and L the orbit length.

When the BPM measures the relative shift of the beam, connected with the voltage difference between the opposite electrodes $U_1 - U_2$, one can see that by changing the capacitance of the electrodes to ground we will be able to tune to zero the differential signal for the equilibrium beam position in horizontal and vertical directions, independently from the initial alignment of the pickup electrodes. This approach allows us to use the so-called "zero-method" for measurements.

All electrodes are connected with charge-sensitive amplifiers. The sum of these signals is used for a measurement of the total beam charge, whereas the difference gives a rough estimation of the beam position. The relative voltage between opposite plates is measured for precise position estimation by two completely insulated from ground, low-noise charge-sensitive amplifiers with integration time sufficiently greater than the betatron oscillation period. These amplifiers measure the beam shift from "zero" position. Using this system the procedure of the beam shift caused by the applied electric field looks like this: One injects the deuteron beam with fixed energy in the ring without electric field. By varying the magnetic-field and the variable capacity one can reach zero signal from precise amplifiers. Then we switch on the radial electric field and inject the deuteron beam with the same fixed energy. You can reach the same "zero" position in radial direction by changing magnetic field. A parasitic vertical component of the electric field will push the equilibrium orbit in the vertical direction and will be measured by the precise charge sensitive amplifiers connected to the vertical plates.

The estimated sensitivity is $dU/dx \approx Ql/(L\,c\,a)$ with a the half of aperture, and c the integral capacity of the electrodes.

Using modest low-noise amplifiers developed at B.I.N.P./Russia with $5\,\text{nV}/\sqrt{\text{Hz}}$ noise and integrated time 1ms we will have 100nV noise. The final sensitivity for single measurement for $a = 5$ cm, $l = 1$ m, $L = 50$ m, $c = 400$ pF, and assuming a modest number of deuterons of 10^9 is about 1 micron. The noise limitation of sensitivity is decreasing as sqrt(number of measurements), and for 0.1 μm we would need 100 pulses or 20s at 5 Hz. The final accuracy will be limited by systematic errors.

Systematic error sources include:

1. During injection or rejection some particles may fall to pickup electrodes and produce a parasitic signal

2. The change of magnetic field magnitude may change the distribution of deuterons, etc.

7 Cost and Schedule

The cost of a dedicated EDM experiment is only incremental over the current g-2 experiment since the bulk of the equipment is going to be used as is. A rough estimate of the extra cost is about 5.4 million dollars with most of the money needed is for the new target with the lithium lens ($1000 K), beam transport line ($415 K) and installation ($390 K), detectors ($400 K), vacuum chambers ($400 K), new inflector ($100 K), ring modification ($400 K), and electrostatic plates with feedback system ($1000 K). A 30% overall contingency is $1.05 M bringing the total to $5.4 M for the experiment completion.

The present muon g-2 experiment is accumulating data according to schedule. If this continues as planned, it is anticipated to take data until the year 2001. In the meantime we would be building a prototype of the electrostatic plates, monitoring system with the laser interferometer and the deuteron polarimeter.

The schedule for the muon EDM is given below:

- Stage I: First we run with polarized deuterons with weak magnetic focusing without modifying the pole pieces of the g-2 ring. At this point we measure the misalignment (with deuterons) and time stability (with laser interferometers) of the $\vec{E}$ field and the orthogonal plane to $\vec{B}$ field to 10 nrad.

- Stage II: Next we run with muons and set a first limit of $10^{-22}\,\mathrm{e}\cdot\mathrm{cm}$, controlling the systematics 100 times better, in 400 hours.

- Stage III: Finally we modify the g-2 pole pieces to store more muons and reach $10^{-23}\mathrm{e}\cdot\mathrm{cm}$ in 4000 hours.

- Stage IV: If the claimed sensitivities can be accomplished and the experiment is statistics limited then we will apply the techniques pioneered by the muon collider, muon storage ring, and the meco collaborations to improve the limit down to 10^{-24} e $\cdot$ cm by injecting 100 times more muons.

8 Summary

We have proposed to search for an EDM of the muon by performing a dedicated experiment in the existing g-2 ring. The main differences from the g-2 experiment are that we are going to place the detector calorimeters inside the vacuum chambers, use magnetic focusing (start with weak and continue with strong later on) with no vertical electric fields present, lower momentum muons, and a lithium lens target with modified beam transport and inflector system. The introduction of an inclinometer, i.e. a system of measuring in situ the misalignment of the average radial electric field direction (which is used to cancel the spin motion of the muon) and the orthogonal to the direction of the average dipole magnetic field. This is done by injecting polarized deuterons in the ring and observe their vertical spin precession as a function of time. Finally, the introduction of a monitoring system of the above alignment of the electric and magnetic field directions by a set of laser interferometers in between the deuteron runs.

The estimated sensitivity is at the level of 10^{-24} e $\cdot$ cm, an improvement of a factor of almost 10^5 to 10^6 over the last CERN muon g-2 experiment, with comparable improvement on the systematic errors.

References

[1] Y.K. Semertzidis *et al.*, Letter of Intent to BNL (1997)

[2] Y.K. Semertzidis, in: Frontier Tests of Quantum Electrodynamics and Physics of the Vacuum E. Zavattini, D. Baklanov and C. Rizzo (eds.), p. 369 (1998)

[3] W. Bernreuther and A. Suzuki, Review of Modern Physics **63**, 313 (1991)

[4] D. Chang, W.Y. Keung and A. Pilaftsis, Phys. Rev. Lett. **82**, 900 (1999); A. Pilaftsis, Phys.Rev. **D58**, 96010 (1998)

[5] C.G. Geng and J.N. Ng, Phys. Rev. **D 42**, 1509 (1990)

[6] V. Barger, A. Das, C. Kao, Phys. Rev. **D 55**, 7099 (1997)

[7] D. Bowser-Chao, D. Chang, W. Keung, Phys. Rev. Lett. **79**, 1988 (1997)

[8] W. Molzon *et al.*, MECO Proposal to the Brookhaven National Laboratory (1998)

[9] T. Mori *et al.*, Proposal R-99-05 to Paul Scherrer Institut, Villigen, Switzerland (1999)

[10] R.M. Carey *et al.*, Phys. Rev. Lett. **82**, 1632 (1999)

[11] C.Caso *et al.*, Eur. Phys. Jour. **C3**, 1 (1998)

[12] S.M. Barr and W. Marciano, in CP Violation, ed. C. Jarlskog, World Scientific, Singapore (1989)

[13] I.B. Khriplovich and M. Pospelov, Nucl. Phys. **B 420**, 505 (1994); F. Hoogevenn, Nucl. Phys. **B341**, 322 (1990); I.B. Khriplovich, Phys. Lett. **B 173**, 193 (1986)

[14] N. Ramsey, at "Breit Symposium", Yale (1999)

[15] P.G.H Sandars, Phys. Rev. Lett., **19**, 1396 (1967)

[16] S. Dimopoulos and L.J. Hall, Phys. Lett. **B344** (1995)

[17] R.Barbieri, A. Romanino and A. Strumia, Phys. Lett. **369**, 283 (1996)

[18] E.D. Commins *et al.*, Phys.Rev. A**50**, 2960 (1994); see also: E.A. Hinds and B.E. Sauer, Physics World **10**, 37 (1997)

[19] J. Bailey *et al.*, Nucl. Phys. B**150**, 1 (1978); J. Bailey *et al.*, Nucl. Phys. **B150**, 1 (1979); F.J.M. Farley and E. Picasso, in Quantum Electrodynamics, ed. T. Kinoshita, World Scientific, Singapore p. 479 (1990)

[20] M. Aciari, *et al.*, Phys. Lett. **B** , (1998)

[21] D. Cho et al. Phys. Rev. Lett. **63**, 2559 (1989); see also: H.M. Quiney *et al.*, Phys.Rev. A **57**, 920 (1998)

[22] P.G. Harris *et al.*, Phys. Rev. Lett. **82**, 904 (1999); see also: S.K. Lamoreaux and R. Golub, Phys. Rev. **D 61**, 051301 (2000)

[23] L.I. Schiff, Phys.Rev. **132**, 2194 (1963)

[24] P.G.H. Sandars, Workshop on Nuclear electric Dipole Moment Searches, GSI, Darmstadt (1999)

[25] I.B. Khriplovich, S.K. Lamoreaux, "CP Violation without Strangeness", Springer, Berlin (1997)

[26] J.P. Jacobs *et al.*, Phys. Rev. **A 52**, 3521 (1995)

[27] D. DeMille and B. Sauer, Workshop on Nuclear electric Dipole Moment Searches, GSI, Darmstadt (1999)

[28] V.W. Hughes, W.M. Morse, B.L. Roberts *et al.*, AGS Experiment E821 at the Brookhaven National Laboratory, Design Report (1995)

[29] A. Weis *et al.*, in: Atomic Physics Methods in Modern Research, Lecture Notes in Physics **499**, Springer, Berlin, p. 57 (1997)

[30] R. Grimm, priv. comm. (1998)

[31] I.B. Khriplovich ,Phys. Lett.**B 444**, 98 (1998); I.B. Khriplovich, talk at PANIC99, (1999)

[32] A. Pilaftsis, Workshop on Nuclear electric Dipole Moment Searches, GSI, Darmstadt (1999)

[33] K.S. Babu *et al.*, Phys. Rev. **D59**, 016004 (1998)

[34] T. Ibrahim and P. Nath, hep-ph/9907555

[35] U. Chattopadhaya and P. Nath, Phys. Rev. **D53**, 1648 (1996)

[36] T. Moroi. Phys. Rev. **D53**, 6565 (1996)

[37] D. Hertzog *et al.*, in Particles Strings and Cosmology, ed. P. Nath, World Scientific, p. 168 (1999)

[38] T. Kinoshita and W.J. Marciano, in Quantum Electrodynamics, ed.T. Kinoshita, World Scientific, Singapore, p. 419 (1990)

[39] W. Marciano, HISMUS Workshop, Tsukuba (1999)

[40] B.L. Roberts, Lepton Photon conference 1999 (hep-ex/0002005)

[41] W. Marciano, Lepton Moments Workshop, Heidelberg (1999)

[42] F.J.M. Farley and E. Picasso, "Quantum Electrodynamics", ed. by T. Kinoshita (World Scientific, Singapore, 1990), p. 479

[43] C.L. Wang, Phys. Rev. **7**, 2609 (1993)

[44] H.N. Brown, Private Communication

[45] F. Krienen, D. Loomba, W. Meng, NIM **A283**, 5 (1989); F. Krienen, D. Loomba, W. Meng, "Development of Non-ferrous Superconducting Magnets", Muon g-2 Note #63

[46] Yuri Orlov, "Spin and Beam Dynamics I", muon g-2 note #279

[47] J. Miller, R. Carey, and E. Hawk, "Measurement of the Muon Electric Dipole Moment in E821", muon g-2 note #215

[48] V. Radeka, private communication

[49] Specs provided by Agilent Technology (HP subsidiary) for their system

[50] K. Hatanaka *et al.*, Nucl. Phys. **A426**, 77 (1984)

[51] S.P. Wells *et al.*, Nucl. Instrum. and Methods **A325**, 205 (1993)

[52] H. Witała *et al.*, Few-Body Systems **15**, 67 (1993)

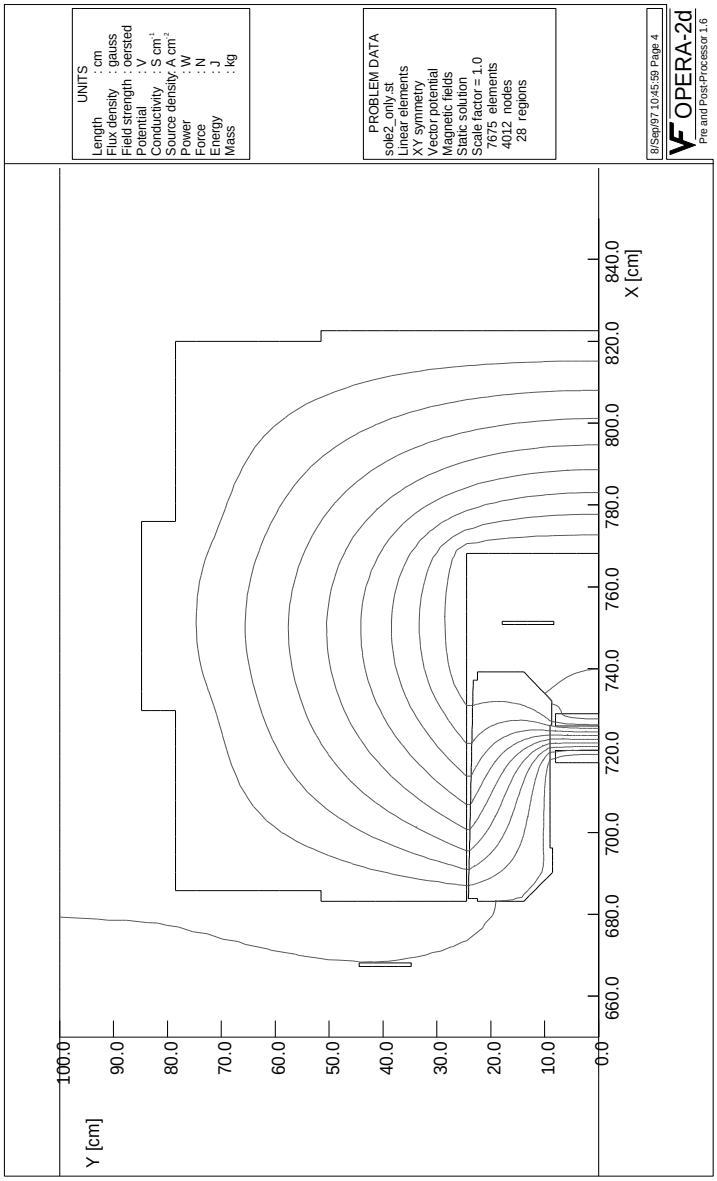

Figure 2: The proposed new inflector design for the EDM experiment located at 723 cm away from the center of the $g-2$ ring. The muon storage center is at 711.2 cm. The magnetic flux lines are shown with only the inflector energized.

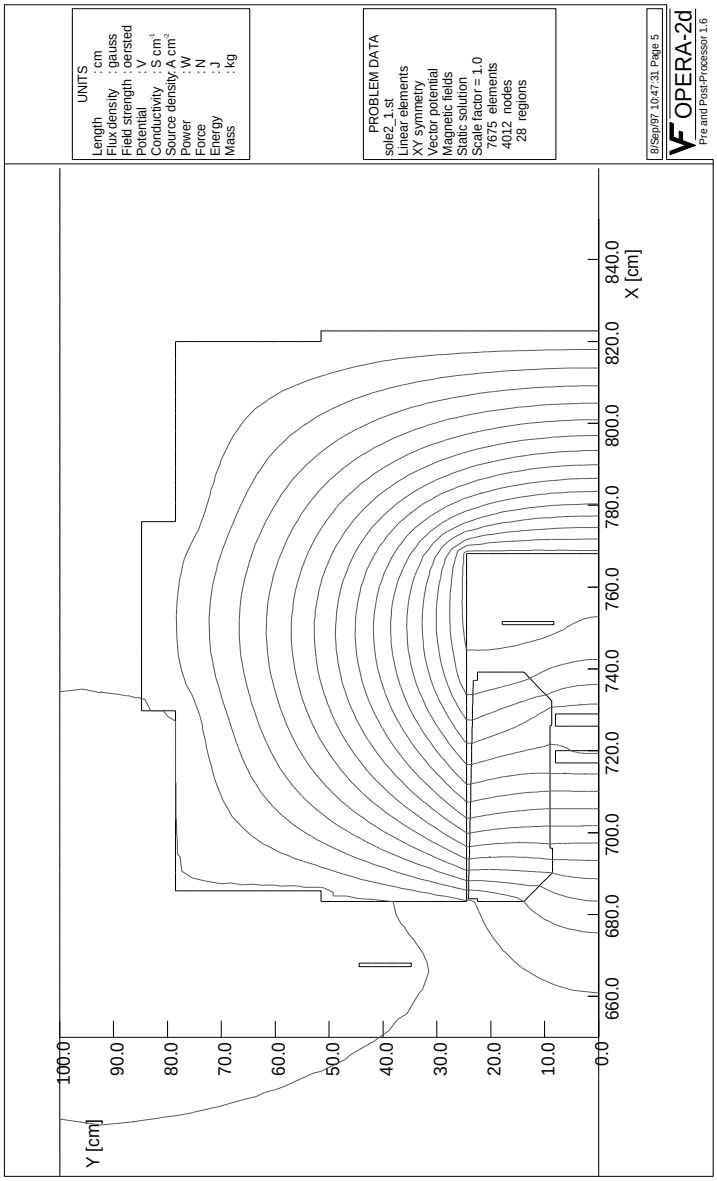

Figure 3: The magnetic flux when both the main magnet and the inflector are powered. The required current density for no magnetic field inside the inflector is 31.7 KA − turn.

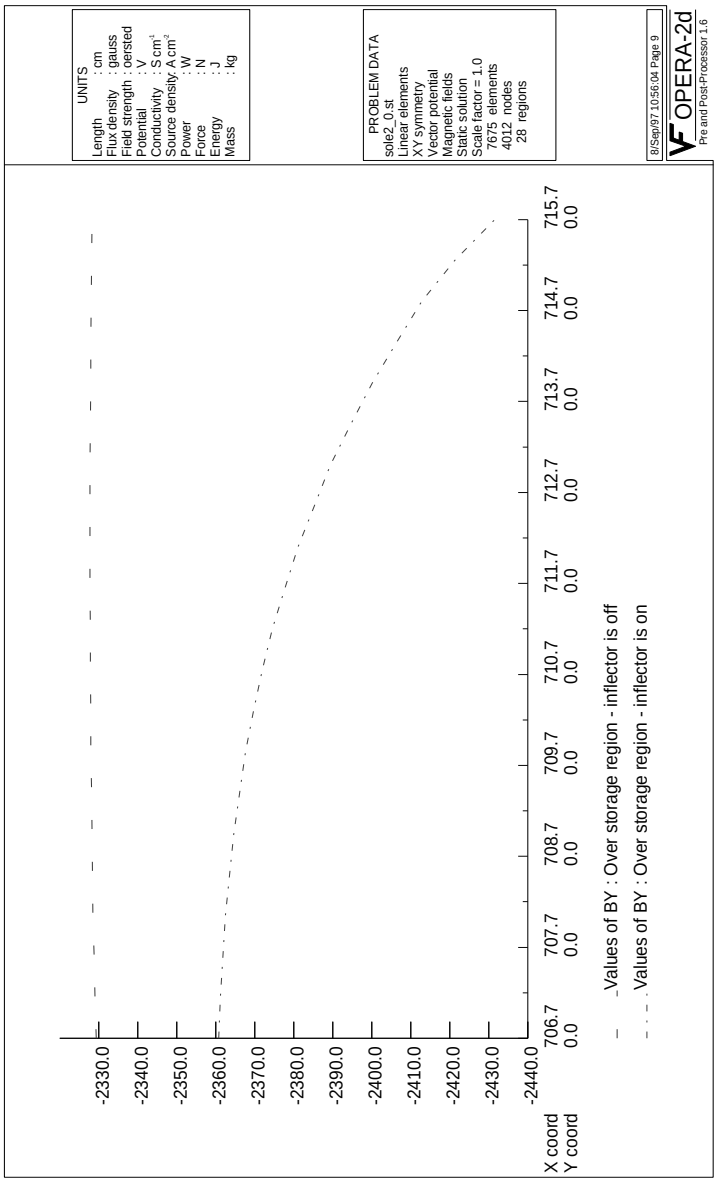

Figure 4: The vertical magnetic field in gauss at the location of the muon storage region with and without the inflector energized.

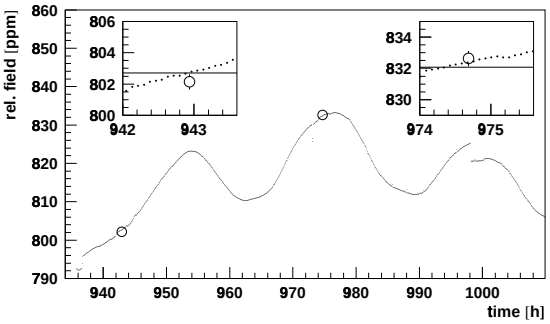

Figure 5: The average magnetic field over a period of about three days during the 1997 run. The inserts indicate measurements with the beam tube trolley.

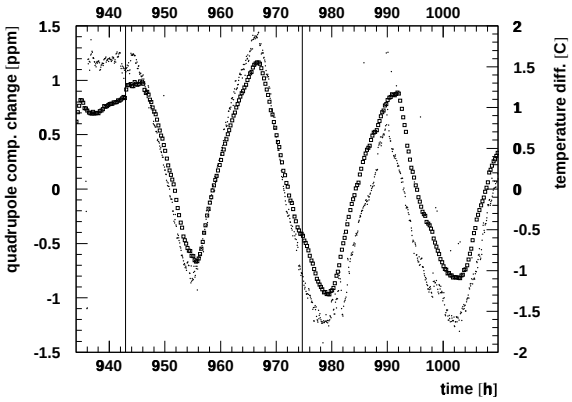

Figure 6: Temperature difference between the magnet yoke surface and the experimental hall temperature (squares) and the change of the normal quadrupole component (dots) during the same time interval.

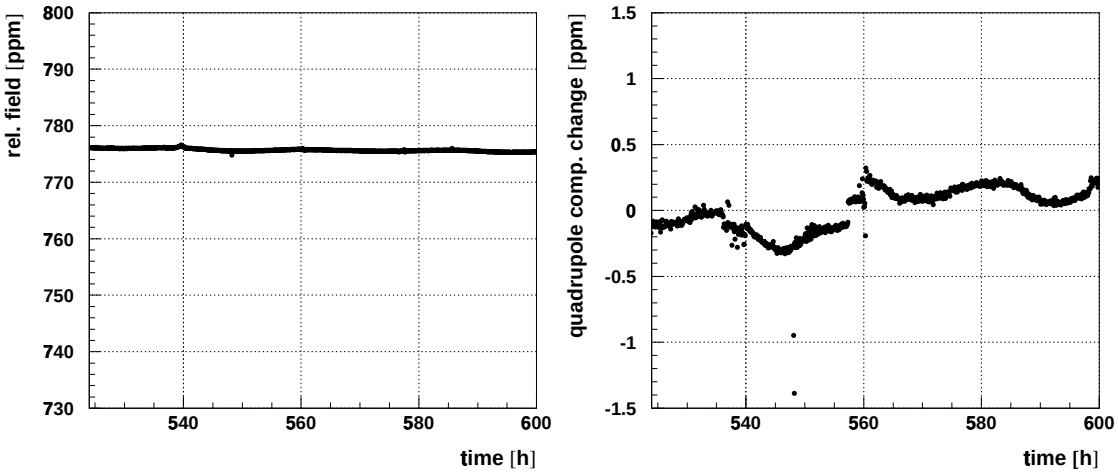

Figure 7: The average magnetic field (left) and normal quadrupole component (right) over a period of about three days during the 1998 run.

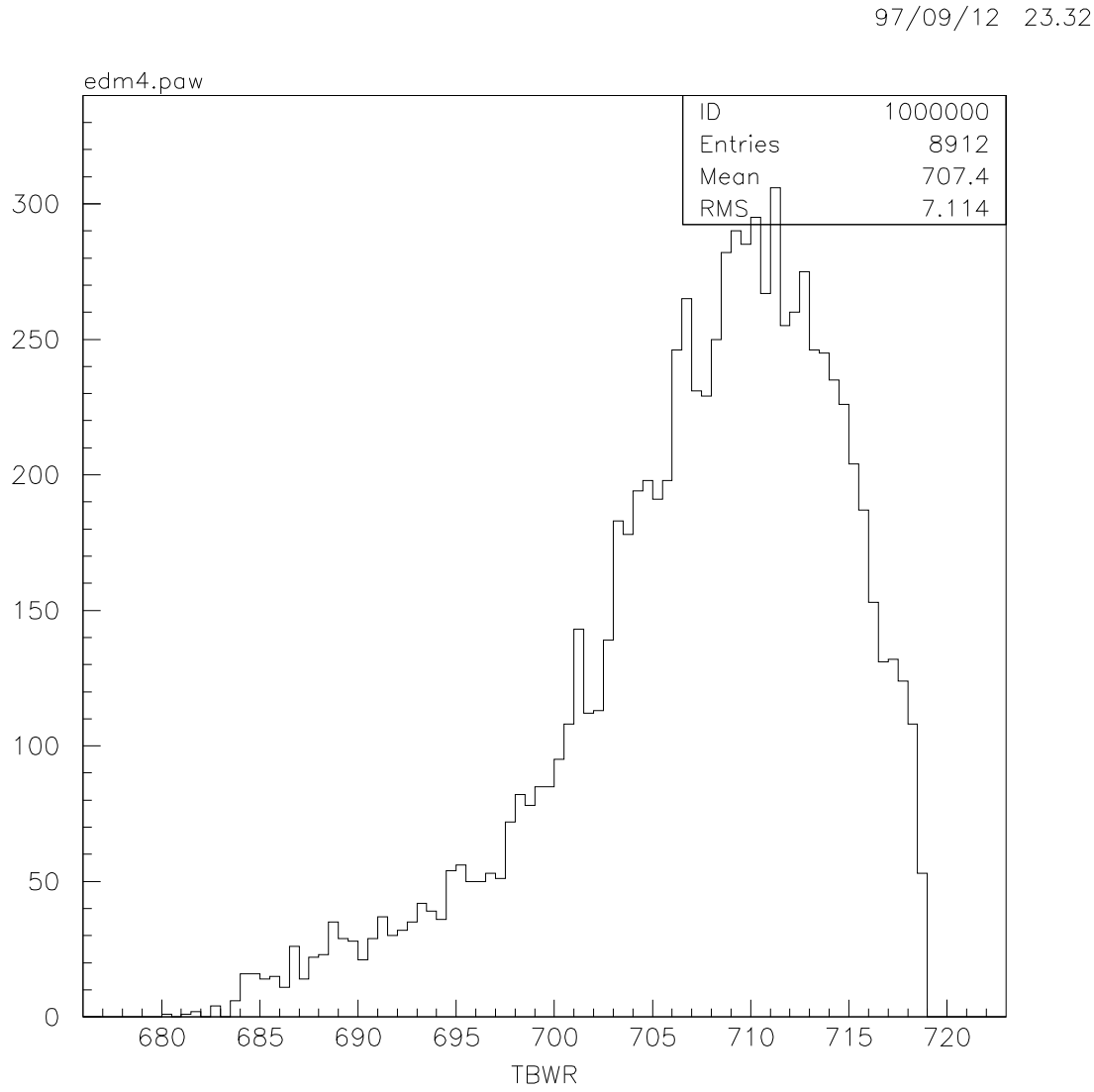

Figure 8: The distribution of the radial position of the decay electrons when they strike either a top or bottom detector. The radius is to be compared with the central storage radius of 7.11 m. The peak is at a slightly smaller radius than 7.11 m.

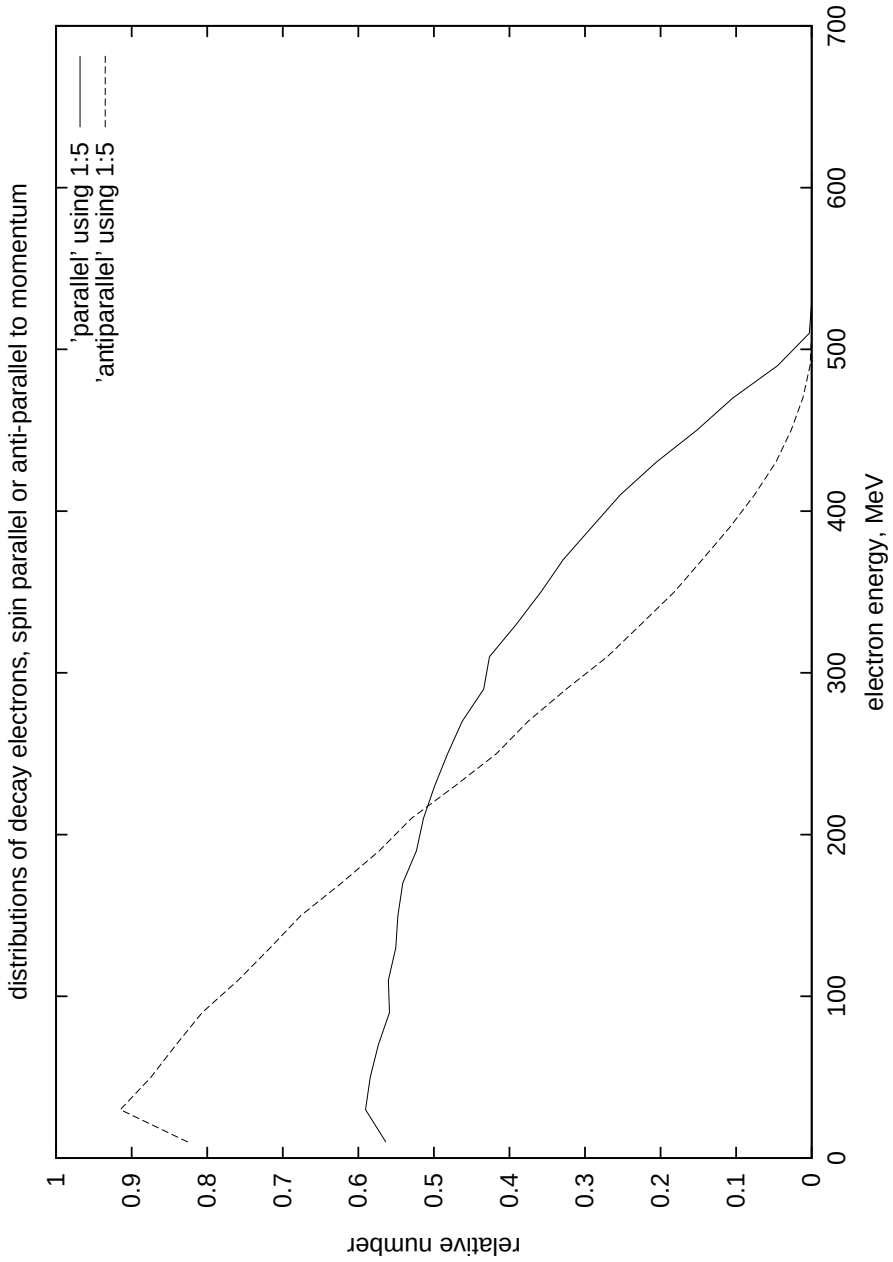

Figure 9: The decay electron energy distributions for forward and backward muon spins.

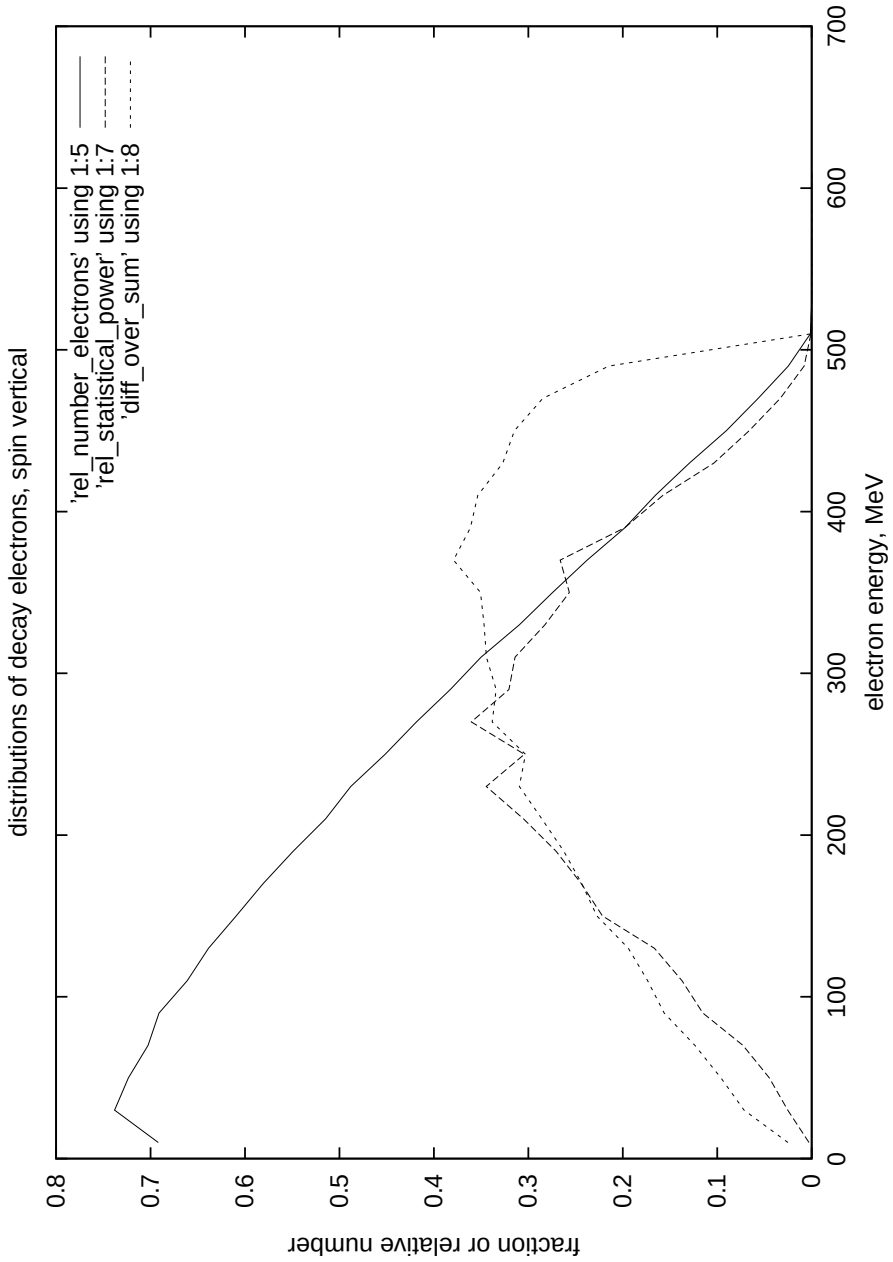

Figure 10: The number of decay electrons vs energy which strike the detector, the up-down asymmetry=$\frac{N_{up}-N_{dn}}{N_{up}+N_{dn}}$, and the relative statistical power of the electron data, which is proportional to the inverse of the relative error on the up-down asymmetry. The most statistically significant electrons are those with energies above 100 MeV, with a peak around 275 MeV. The energy distribution shown is for vertically oriented spin, which gives a distribution somewhere between the energy distribution for forward and backward muon spins.

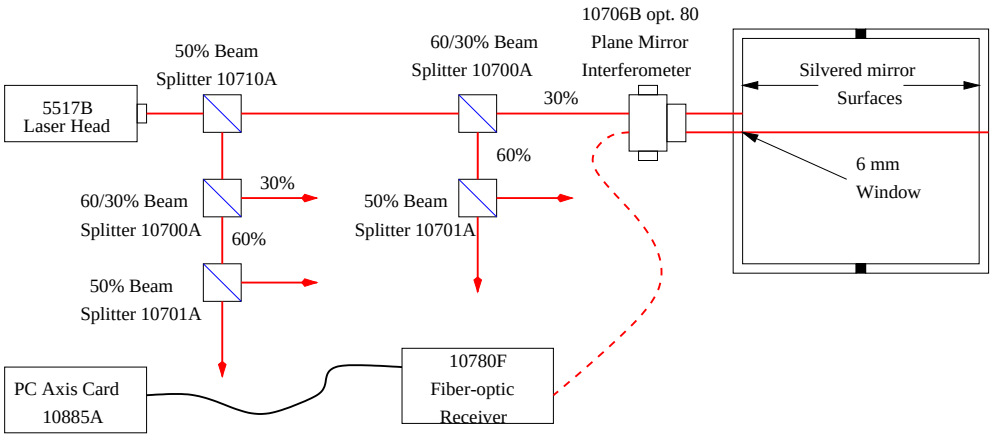

6 Axis per Laser Head

The plane mirror interferometers 10706B will measure the change in spacing of the 2 silvered surfaces. The detailed optical layout for all 40 measurement axis is done by the integrater. Other optical components such as Beam Benders 10707A and Adjustable Mounts, 10710A & 10711A, are available to aid in layout and alignment.

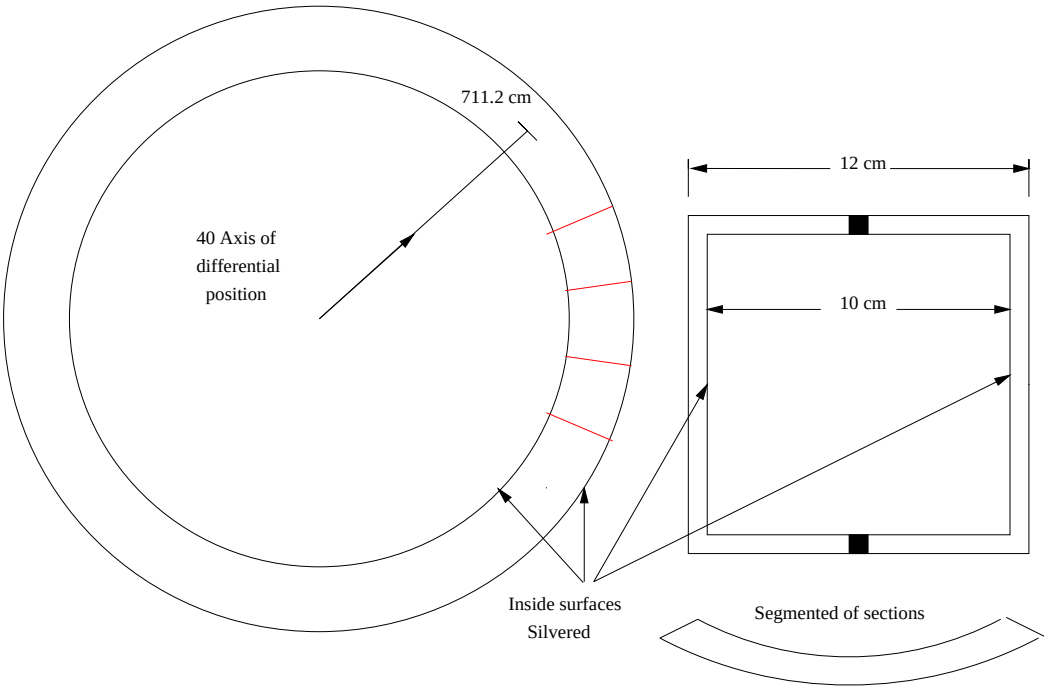

Figure 11: The cross section of the plates (10 cm by 10 cm) is shown on the right. The top and bottom plates consist of conductive glass plates. On the top of the figure the laser interferometer is shown which has 5 nm relative position resolution with 33 KHz response speed.